Supplement for "The impact of circulation patterns on regional transport pathways and air quality over Beijing and its surroundings"

J. P. Zhang[1], T. Zhu[2], Q. H. Zhang[1], C. C. Li[1], H. L. Shu[1], Y. Ying[1], Z. P. Dai[3], X. Wang[1], X. Y. Liu[1], A. M. Liang[4], H. X. Shen[4] and B. Q. Yi[5]

[1]Department of Atmospheric and Oceanic Sciences, School of Physics, Peking University, Beijing, China

[2]State Key Joint Laboratory of Environmental Simulation and Pollution Control, College of Environmental Sciences and Engineering, Peking University, Beijing, China

[3]Shenzhen Academy of Environmental Science, Shenzhen, China

[4]Meteorological Center of North China Air Traffic Management Bureau of CAAC, Beijing, China

[5]Department of Atmospheric Sciences, Texas A&M University, College Station, TX 77845, USA

Correspondence to: J. P. Zhang (zhangjp@pku.edu.cn), Q. H. Zhang (qzhang@pku.edu.cn)

S1. WRF Domains

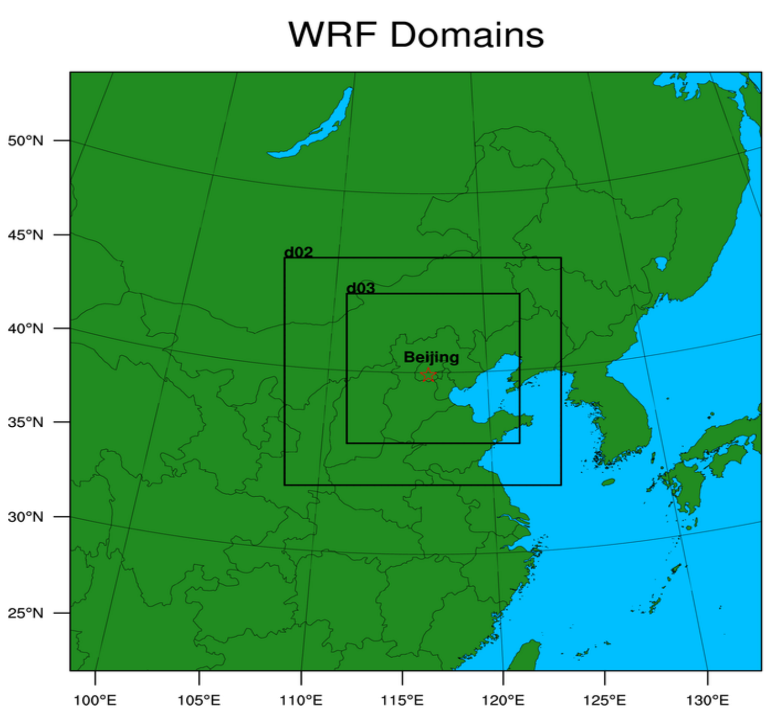

Figure S1. WRF domains 1-3.

S2. Comparison of WRF outputs with the in-situ observations.

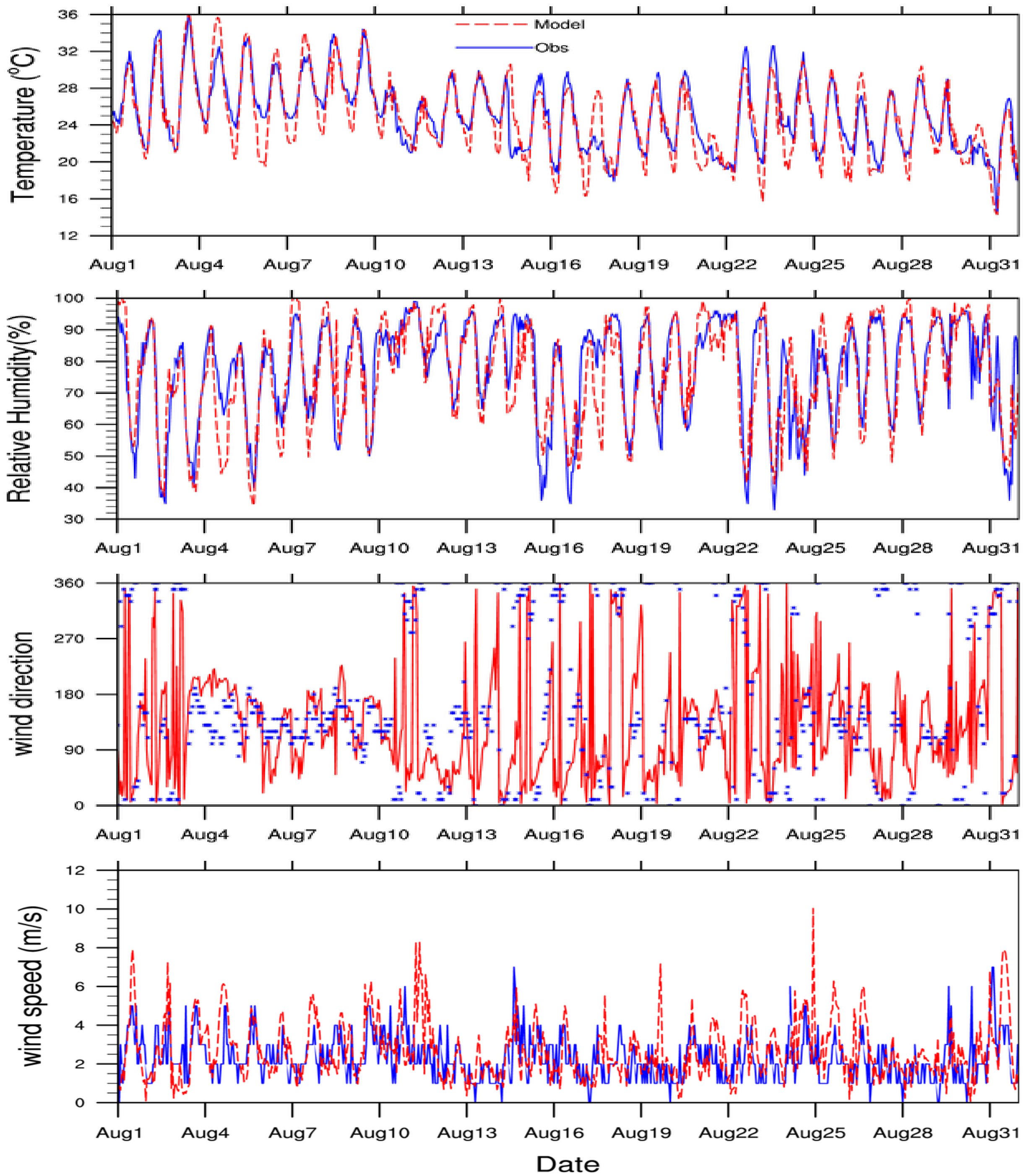

Figure S2(a). Comparison of model hourly outputs from 4 km WRF simulation (red line) with observed hourly temperature, relative humidity (at 2 m), wind speed and wind direction at 10 m (blue line or dot) at Beijing Capital International Airport (40.06°N, 116.58°E) for August 2008.

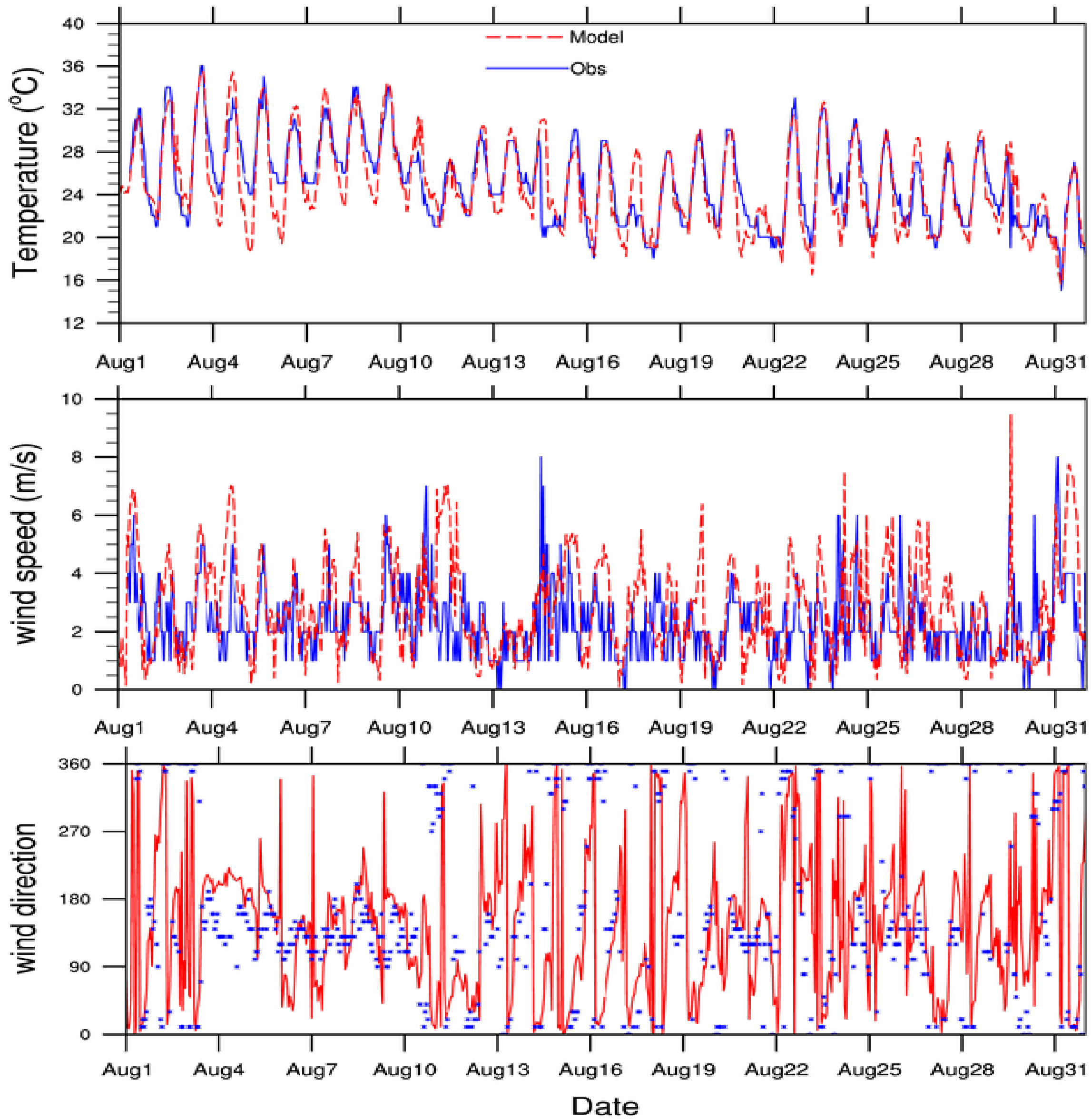

Figure S2(b). Time series of observed and WRF-simulated (red line) hourly averaged temperature (a), relative humidity (b), wind speed (c), and wind direction (d) at Beijing Observation site (WMO 54511; 39.9°N, 116.3°E) for August 2008.

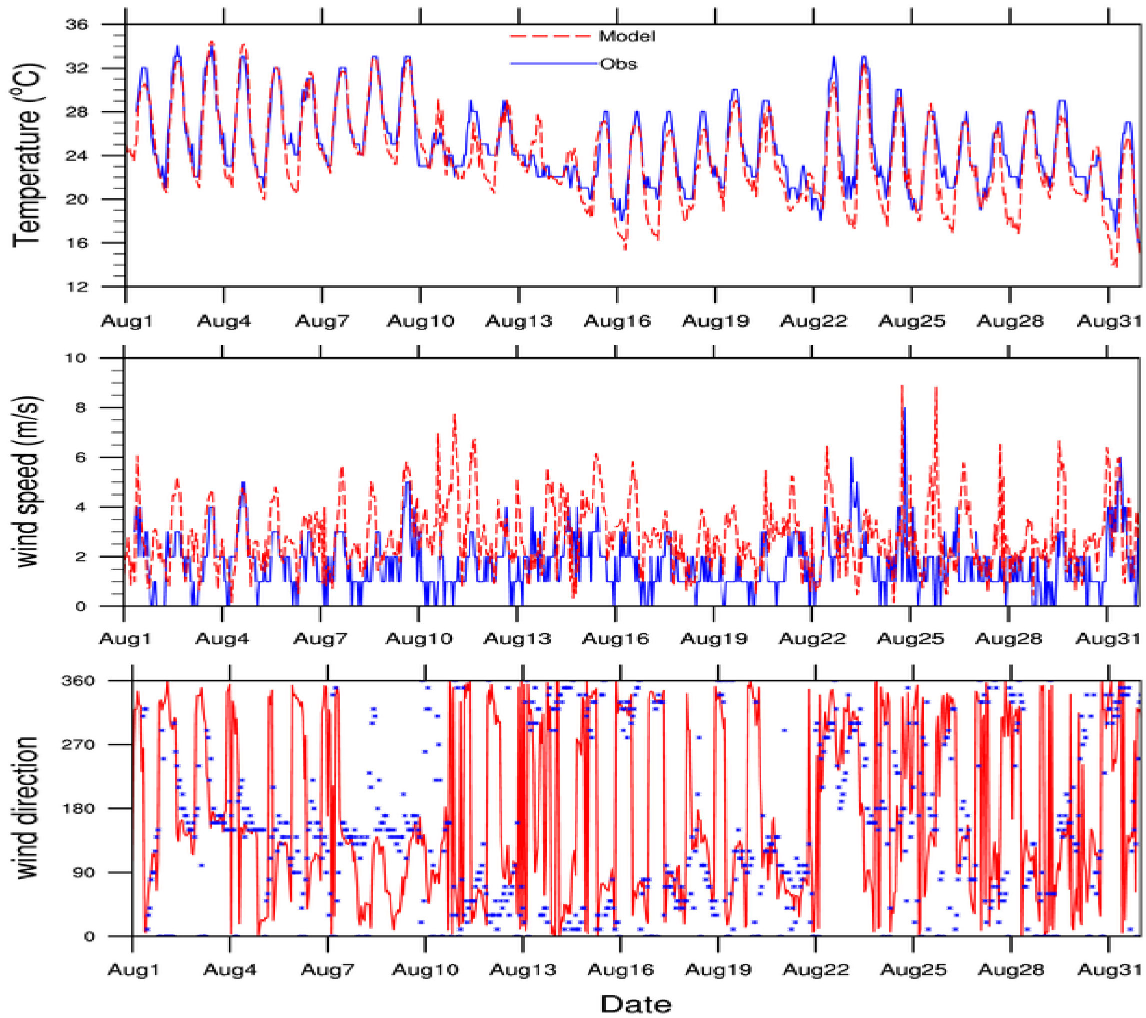

Figure S2(c). Time series of observed and WRF-simulated (red line) hourly averaged temperature (a), relative humidity (b), wind speed (c), and wind direction (d) at Shijiazhuang site (38.3°N, 114.7°E) for August 2008.

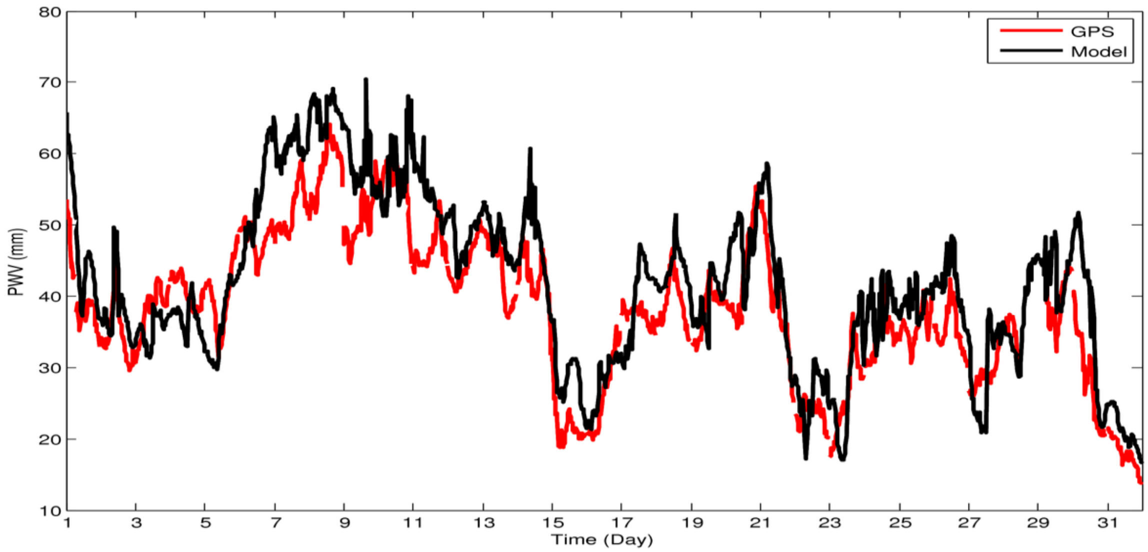

Fig. S3. Time series of observed and simulated half-hourly column-integrated Precipitable Water Vapor (PWV) at PKU site during August 2008. The GPS-based water vapor (data source: http://www.suominet.ucar.edu/support/) is shown in red line, and the black line denotes WRF-simulated water vapor (Domain 3). The correlation=0.884, mean error =3.62 mm, bias =3.5mm.

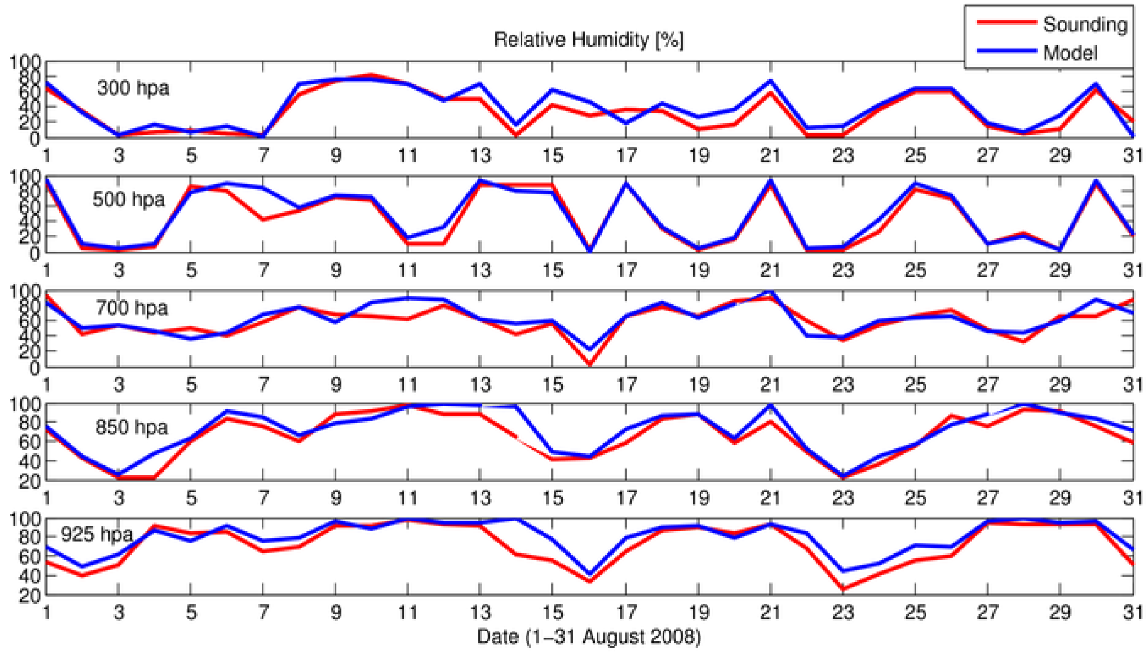

Fig. S4(a). Time series of observed (red lines) and simulated (24h forecasting; blue lines) daily relative humidity of sounding at Beijing Observational site. The bottom-up levels are 925, 850, 700, 500, and 300 hPa, respectively.

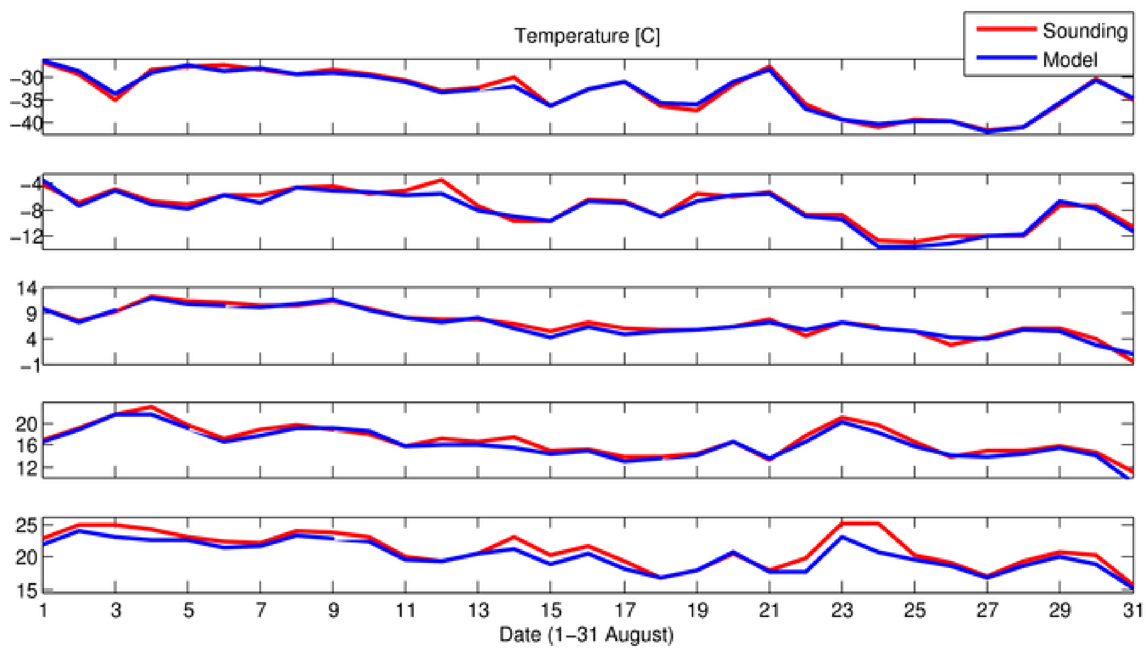

Fig. S4(b). The same as Fig. S4(a), but for temperature.

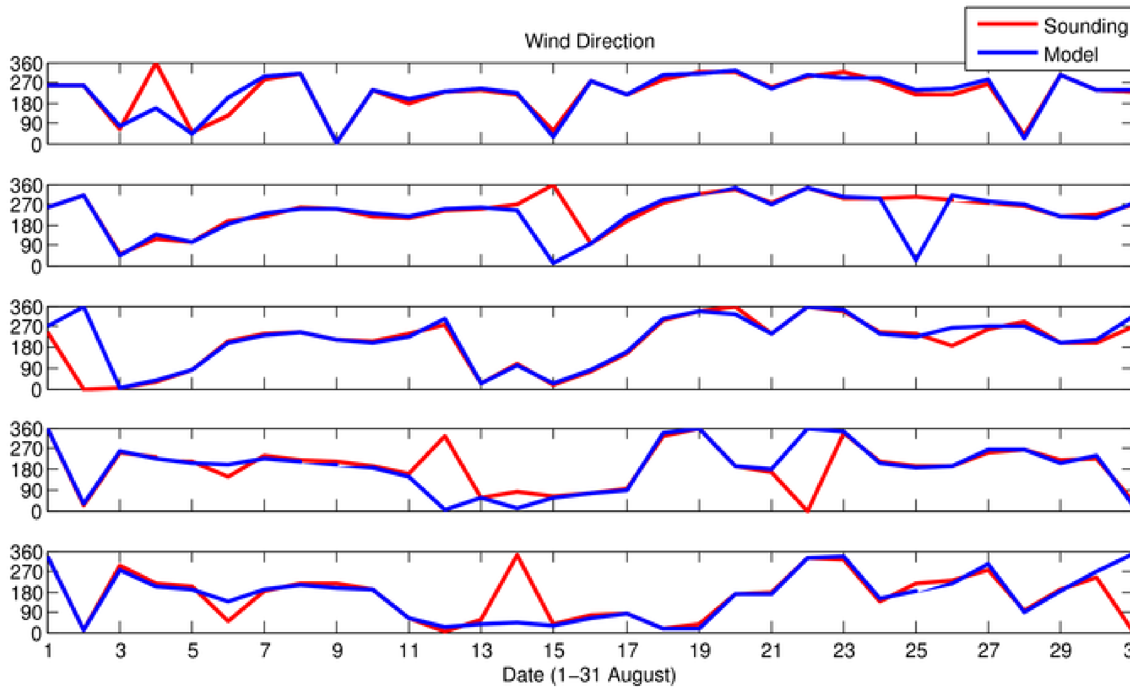

Fig. S4(c). The same as Fig. S4(a), but for wind direction.

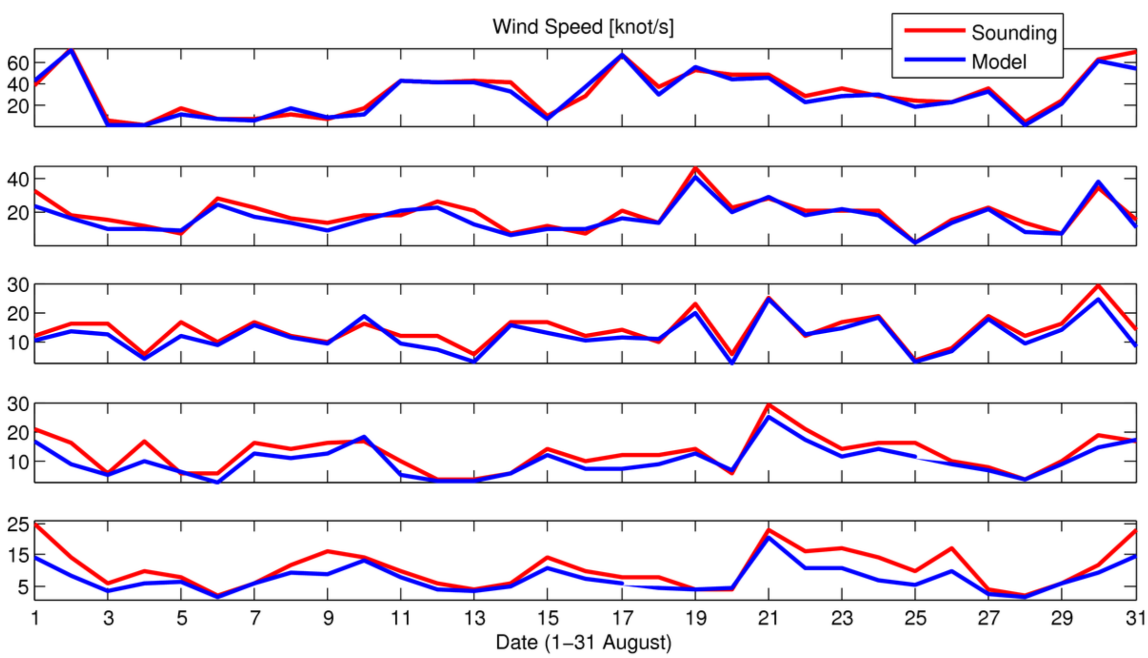

Fig. S4(d). The same as Fig. S4(a), but for wind speed.

S3. Time serials of data availability.

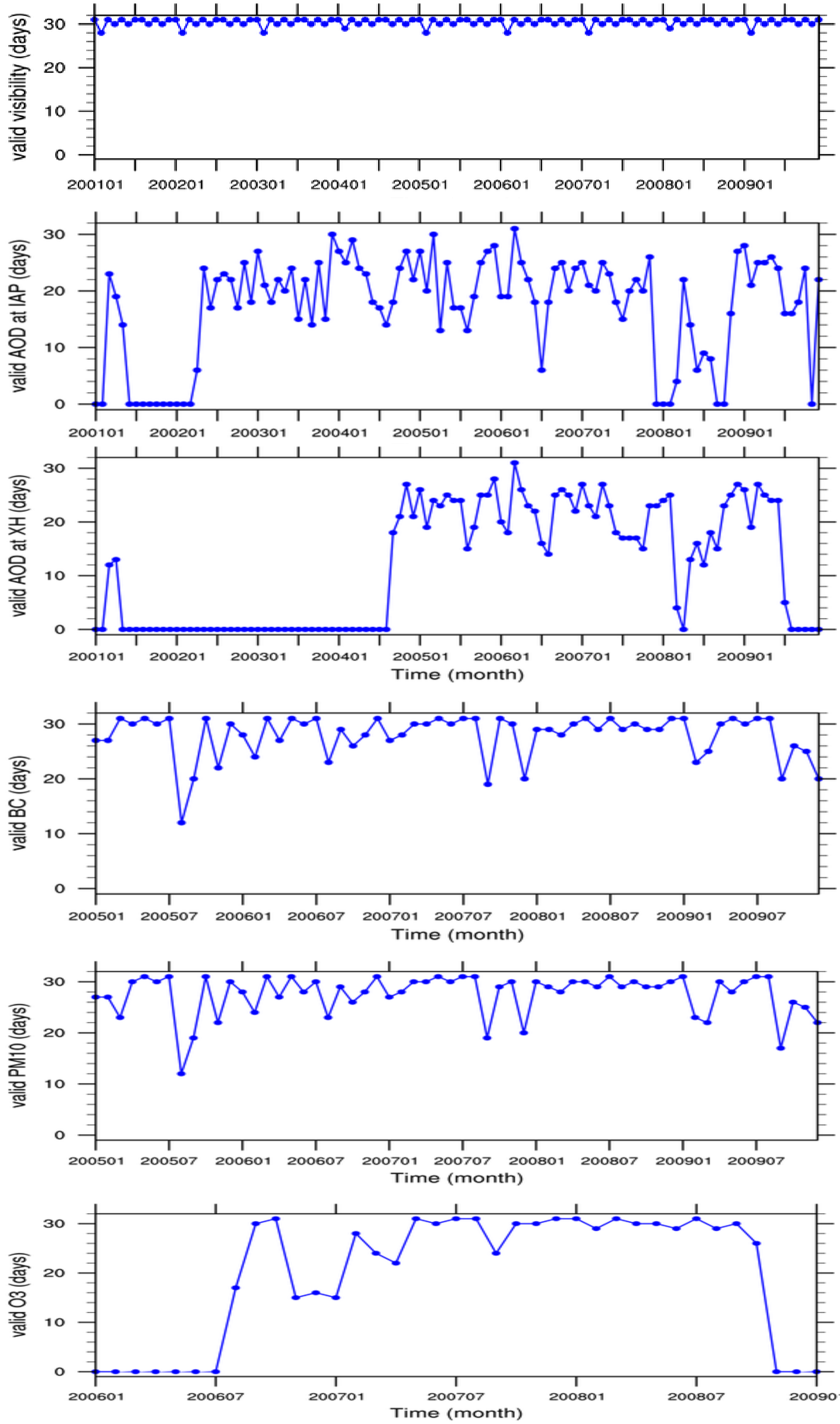

Fig. S5. Monthly time series of valid daily data numbers for (a) AOD at IAP, (b) AOD at XH, (c) BC, (d) PM10, and (e) O3. The other gas species are similar to O3. There is no missing data in meteorological variables at BCIA.

S4. Examples for footprint map of backward plume trajectories.

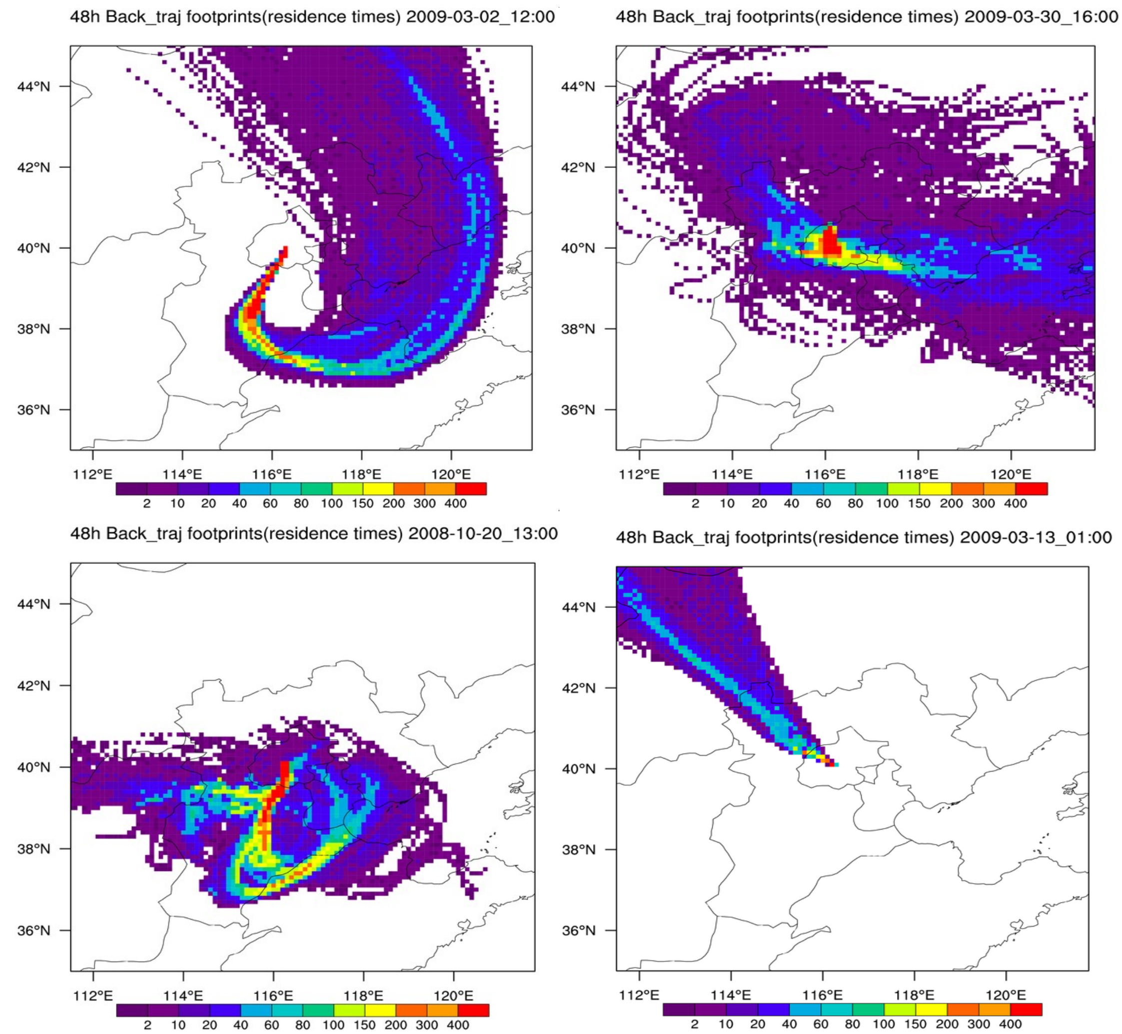

Fig. S6. Examples of footprint map of 48-h plume backward trajectories released at specific times (UTC) from PKU site.

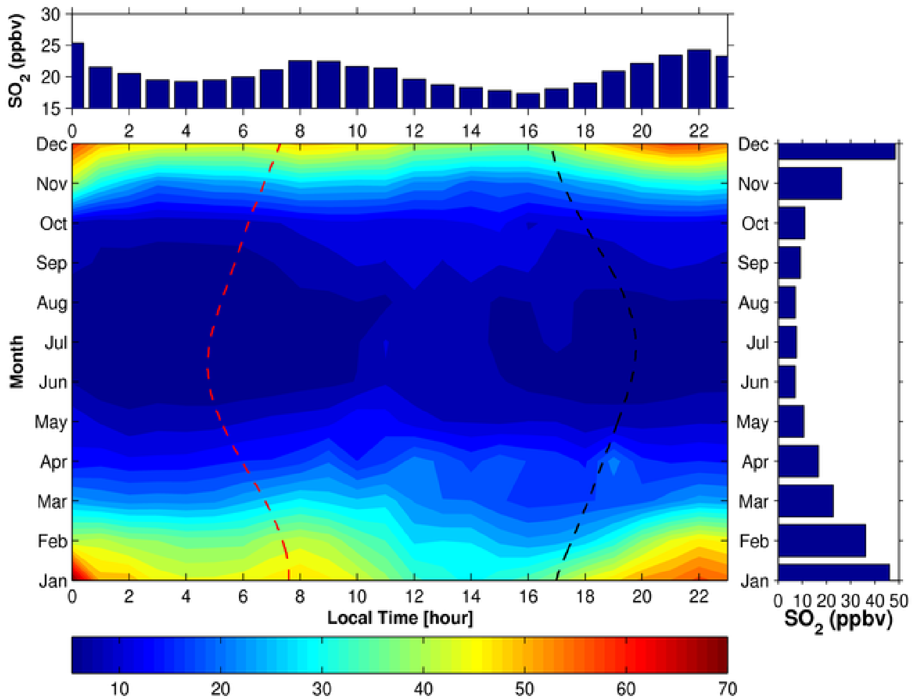

Fig. S7. SO_2 concentration distribution in relation to month and local time (filled color; unit: ppbv) from August 2006 to Octomber 2008 at PKU site. Red dash line represents sunrise time and black dash line represents sunset time.

S5. 500-hPa geopotential height during the pre-Olympics, Olympics and the period from 21 July to 08 August 2000-2009.

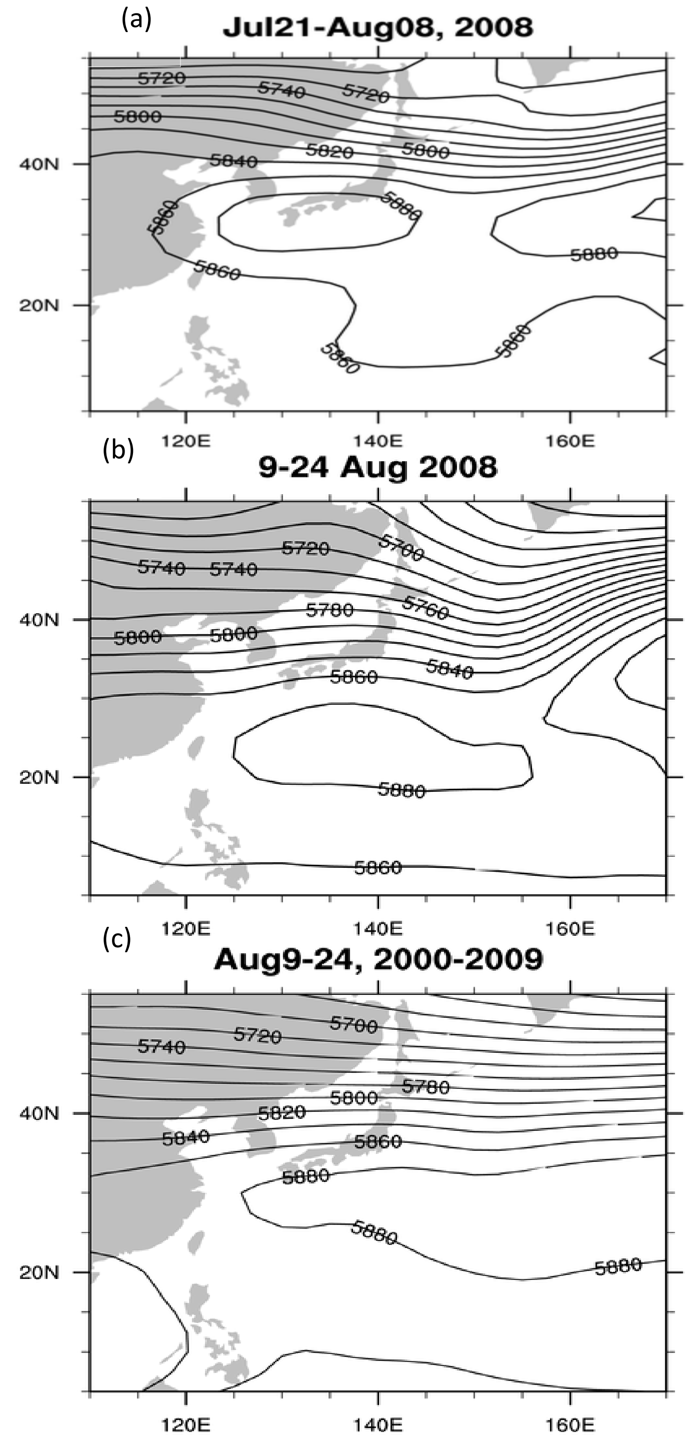

Fig. S8. 500-hPa geopotential height (gpm) during (a) the pre-Olympics (21 July – 08 Aug, 2008), (b) Olympics (09-24 Aug, 2008) and (c) the period from 21 July to 08 August 2000-2009.

S6. Sensitivity studies of the temporal and spatial stability for Circulation Classification.

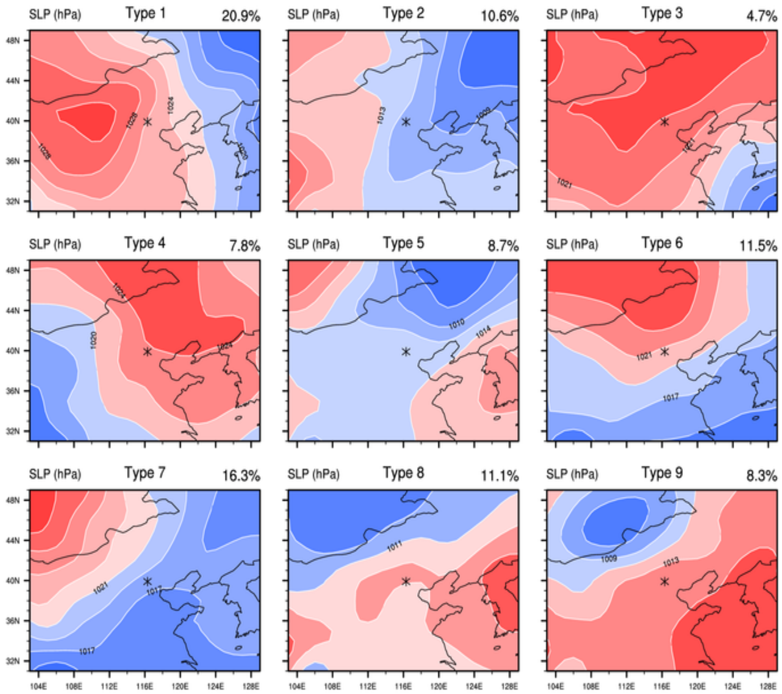

Fig. S9(a). Mean sea level pressure (SLP) patterns and frequency of occurrence (right upper number) for each circulation type during the period 2000 to 2009. The asterisk represents the location of Beijing.

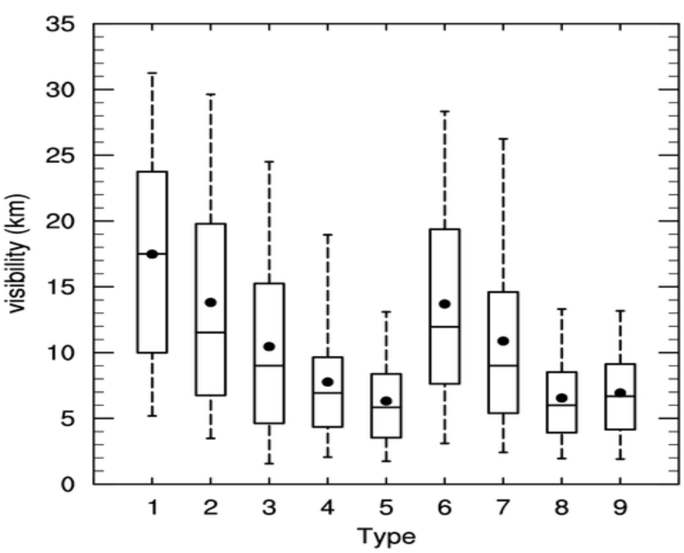

Fig. S9(b). Daily mean visibility at Beijing airport within the nine clusters.

Fig. 9. Experiment 1: changing the predefined domain one degree to south (31-49N).

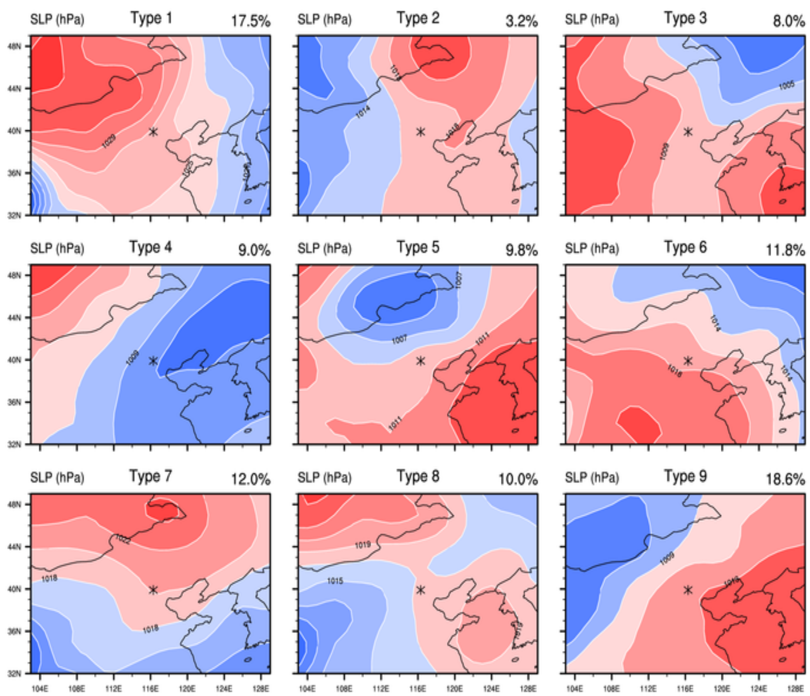

Fig. S10 (a). Mean sea level pressure (SLP) patterns and frequency of occurrence (right upper number) for each circulation type during the period 2000 to 2009. Sensitivity study of adjustment input data as 06:00 UTC (LT 14:00) SLP.

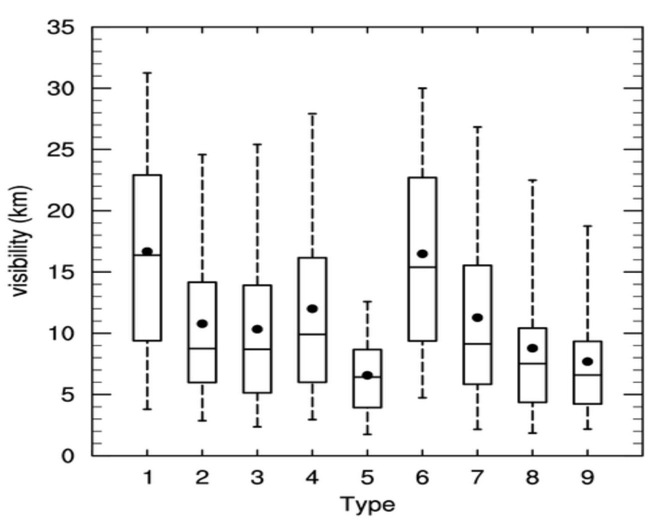

Fig. S10 (b). Daily mean visibility at Beijing airport within the nine clusters.

Fig. 10. Experiment 2: using 06:00 UTC SLP as input data.

S7. Statistical difference of the mean of the meteorological variables among the circulation types.

Table S1. Statistical difference of the mean of the meteorological variables among the different circulation types, at a significance level of 0.05, during 2000-2009.

Circulation type	Temperature	Relative Humidity	Surface Pressure	Wind speed	Cloud cover	Visibility
1	2,3,4,5,6,7,8,9	2,3,4,5,6,7,8,9	2,3,4,5,6,7,8,9	2,3,4,5,6,7,8,9	2,3,4,5,6,7,8,9	2,3,4,5,6,7,8,9
2	1,3,4,5,6,7,8,9	1,4,5,7,8,9	1,3,4,5,6,7,8,9	1,3,4,5,6,7,8,9	1,3,4,6,7,8,9	1,3,4,5,6,7,8,9
3	1,2,4,5,6,7,8	1,4,5,7,8,9	1,2,4,5,6,7,8,9	1,2,4,8,9	1,2,5,6,7,8,9	1,2,4,5,6,7,8,9
4	1,2,3,5,8,9	1,2,3,5,6,7,8,9	1,2,3,5,7,8	1,2,3,5,6,7	1,2,5,6,7,8,9	1,2,3,5,6,8,9
5	1,2,3,4,6,7,8	1,2,3,4,6,7,8,9	1,2,3,4,6,7,9	1,2,4,9	1,3,4,6,7,8,9	1,2,3,4,6,7,8,9
6	1,2,3,5,8,9	1,4,5,7,8,9	1,2,3,5,7,8	1,2,4,8,9	1,2,3,4,5,7,8	1,2,3,4,5,7,8,9
7	1,2,3,5,8,9	1,2,3,4,5,6,8,9	1,2,3,4,5,6,8,9	1,2,4,9	1,2,3,4,5,6,8,9	1,2,3,5,6,8,9
8	1,2,3,4,5,6,7,9	1,2,3,4,5,6,7,9	1,2,3,4,6,7,9	1,2,3,6	1,2,3,4,5,6,7,9	1,2,3,4,5,6,7
9	1,2,4,6,7,8	1,2,3,4,5,6,7,8	1,2,3,5,7,8	1,2,3,5,6,7	1,2,3,4,5,7,8	1,2,3,4,5,6,7

S8. Statistical difference of the mean for the air quality parameters among the circulation types.

Table S2. Statistics of visibility and AERONET AOD for the nine circulation types.

Circulation Type	Visibility (km)				Aeronet AOD (Beijing site)			
	Median	Mean	Std dev	Statistical difference*	Median	Mean	Std dev	Statistical difference*
1	18.73	18.49	8.26	2,3,4,5,6,7,8,9,	0.19	0.28	0.27	2,3,4,5,6,7,8,9,
2	10.62	12.4	7.61	1,3,4,5,6,7,8,9,	0.37	0.57	0.55	1,3,4,5,7,8,9,
3	9.17	11.11	7.68	1,2,4,5,6,7,8,9,	0.57	0.68	0.56	1,2,5,6,8,9,
4	7.97	9.42	5.94	1,2,3,5,6,8,9,	0.51	0.74	0.62	1,2,5,6,8,9,
5	5.61	5.99	3.47	1,2,3,4,6,7,8,9,	1.12	1.21	0.59	1,2,3,4,6,7,8,9,
6	12.45	14.33	8.45	1,2,3,4,5,7,8,9,	0.32	0.53	0.51	1,3,4,5,7,8,9,
7	8.19	9.78	6.51	1,2,3,5,6,8,9,	0.66	0.81	0.60	1,2,5,6,8,9,
8	6.04	6.57	3.73	1,2,3,4,5,6,7,	0.99	1.08	0.61	1,2,3,4,5,6,7,
9	6.35	6.67	3.64	1,2,3,4,5,6,7,	1.05	1.18	0.63	1,2,3,4,5,6,7,

* Statistical difference of the mean visibility and mean of the AOD among the different circulation types, at a significance level of 0.05.

Table S3. Statistics of PM_{10} concentrations and BC concentration ($\mu g\ m^{-3}$) for the nine circulation types.

Circulation Type	PM_{10} ($\mu g\ m^{-3}$)				BC ($\mu g\ m^{-3}$)			
	Median	Mean	Std dev	Statistical difference*	Median	Mean	Std dev	Statistical difference*
1	70.6	90.3	76.3	2,3,4,5,6,7,8,9,	2.94	4.13	3.76	2,3,4,5,6,7,8,9,
2	122	143.2	97.9	1,5,6,	5.15	5.72	3.49	1,3,5,6,8,9,
3	111.2	140.4	106.6	1,5,6,	6.04	7.28	5.36	1,2,6,
4	122.3	142.8	102.3	1,5,6,	5.41	6.25	4.55	1,5,6,8,
5	155.4	173.4	105.8	1,2,3,4,6,7,	7.44	8.44	4.89	1,2,4,6,7,9,
6	90.4	111.7	89.6	1,2,3,4,5,7,8,9,	3.97	4.82	3.44	1,2,3,4,5,7,8,9,
7	109.1	133.2	91.1	1,5,6,8,	5.52	6.47	4.36	1,5,6,8,
8	146.1	158.4	90	1,6,7,	6.62	7.61	4.35	1,2,4,6,7,9,
9	136.2	151.2	93.1	1,6,	6.01	6.74	3.85	1,2,5,6,8,

* Statistical difference of the mean BC and mean of the PM_{10} among the different circulation types, at a significance level of 0.05.

Table S4. Statistical difference of the mean SO_2, NO_2, O_3 and CO mixing ratio for the nine circulation types.

Circulation Type	SO_2 (ppbv)		NO_2 (ppbv)		O_3 (ppbv)		CO (ppmv)	
	Mean	Statistical difference*	Mean	Statistical difference*	Mean	Statistical difference*	Mean	Statistical difference*
1	22.5	2,6,7,8,	29.51	3,5,7,8,9,	46.19	2,5,6,8,9,	1.39	5,7,9,
2	12.5	1,3,4,5,7,9,	33.82	5,6,9,	69.07	1,4,7,	1.32	4,5,7,8,9,
3	20.77	2,6,8,	36.68	1,6,	61.72		1.68	6,
4	21.72	2,6,8,	32.12	5,6,7,9,	49.03	2,5,8,9,	1.7	2,6,
5	21.34	2,6,8,	42.19	1,2,4,6,8,	69.0	1,4,	2.61	1,2,6,
6	11.89	1,3,4,5,7,9,	27.3	2,3,4,5,7,8,9,	60.35	1,	1.2	3,4,5,7,8,9,
7	29.16	1,2,6,8,9,	38.25	1,4,6,	52.32	2,8,9,	2.04	1,2,6,8,
8	12.99	1,3,4,5,7,9,	35.23	1,5,6,	71.49	1,4,7,	1.6	2,6,7,
9	18.78	2,6,7,8,	39.06	1,2,4,6,	70.73	1,4,7,	2.03	1,2,6,

* Statistical difference of the mean SO_2, O_3, CO and NO_2 mixing ratio among the different circulation types, at a significance level of 0.05.

S9. Description of the error calculation method for the effects of air quality parameters in improving air quality during the 2008 Beijing Olympics

Error estimation:

1. Assumption: The air quality parameters for each CT were with lognormal distribution.
2. According to the error propagation formulas, the climatological mean and standard deviation of each air quality parameters were used to calculate the error estimation for evaluating the relative role of circulation types in improving air quality during the Olympic.